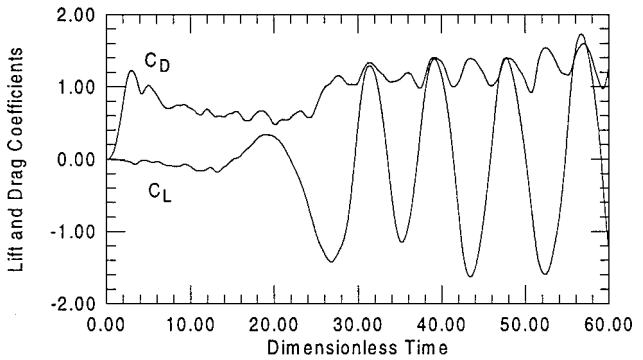

Fig. 2 Variation of C_D and C_L with time for case 9.

Ogami and Ayano[2] computed $C_D = 1.07$, using a Lagrangian viscous vortex method (they did not calculate the Strouhal number). The general agreement between the two numerical methods is acceptable for the mean drag coefficient, and both results are close to the experimental values. However, the three-dimensional and turbulence effects present in the experiments are nonnegligible for the Reynolds number used in the simulations, and a two-dimensional computation must produce higher values for the drag coefficient, as obtained in our simulation.

Conclusions

The vortex method presented here to study the two-dimensional, incompressible, unsteady flow around a fixed circular cylinder is able to predict the main global quantities of a high-Reynolds-number flow. The calculated aerodynamic forces are close to the experimental and numerical data used for comparison. Also, the simulations are able to capture complex flow mechanisms, such as separation, as part of the computation. The analysis of the influence of the numerical parameters on the simulation has pointed out the importance of choosing suitable values for N, Δt, and ε, and the trends when these parameters are varied have also been identified. The numerical results also brought up that ε strongly affects the simulations and, therefore, must be modeled correctly. This is an important output of this work.

Acknowledgments

The authors acknowledge the Conselho Nacional de Desenvolvimento Científico e Tecnológico (National Council for Scientific and Technological Development), under Grants 521260/94-9 and 143041/97-5, and the Fundação de Amparo à Pesquisa do Estado de Minas Gerais (Foundation for Research Support of the State of Minas Gerais), under Grant TEC-1565/97, for the financial support of this project.

References

[1]Chorin, A. J., "Numerical Study of Slightly Viscous Flow," *Journal of Fluid Mechanics*, Vol. 57, Pt. 4, 1973, pp. 785–796.

[2]Ogami, Y., and Ayano, Y., "Flows Around a Circular Cylinder Simulated by the Viscous Vortex Model—The Diffusion Velocity Method," *Computational Fluid Dynamics Journal*, Vol. 4, No. 3, 1995, pp. 383–399.

[3]Sarpkaya, T., "Vortex Element Methods for Flow Simulation," *Advances in Applied Mechanics*, Vol. 31, 1994, pp. 113–247.

[4]Milne-Thomson, L. M., *Theoretical Hydrodynamics*, Macmillan, London, 1968, pp. 157, 158, 255, 256.

[5]Lewis, R. I., *Vortex Element Methods for Fluid Dynamic Analysis of Engineering Systems*, Cambridge Univ. Press, Cambridge, England, U.K., 1991, pp. 372–374.

[6]Blevins, R. D., *Applied Fluid Dynamics Handbook*, Van Nostrand Reinhold, New York, 1984, pp. 313–317.

[7]Greengard, L., and Rokhlin, V., "A Fast Algorithm for Particle Simulations," *Journal of Computational Physics*, Vol. 73, No. 2, 1987, pp. 325–348.

[8]Prasad, A., and Williamson, C. H. K., "Three-Dimensional Effects in Turbulent Bluff-Body Wakes," *Journal of Fluid Mechanics*, Vol. 343, July 1997, pp. 235–265.

J. Kallinderis
Associate Editor

Vibration Analysis of Thick Laminated Composite Cylindrical Shells

K. Y. Lam,* T. Y. Ng,† and Wu Qian‡
National University of Singapore, Singapore 118261, Republic of Singapore

Introduction

THE development of thin-plate and shell theories has received much attention over the past century,[1–3] but only more recently has attention been drawn to thick-plate and shell theories with consideration of transverse shear deformation in multilayered composite plates and shells. Reddy[4] developed a simple higher-order theory for laminated composite plates where the two transverse shear stresses vanish on the top and bottom surfaces and the displacement field is formed by setting the two corresponding strains to zero. Soldatos and Hadjigeorgiou[5] employed the governing equations of three-dimensional linear elasticity and solved them by using an iterative approach for the prediction of the frequencies of vibration.

Voyiadjis and Shi[6] developed a refined higher-order, two-dimensional theory for thick cylindrical shells with very good approximations for the shell constitutive equations and the nonlinear distributions of in-plane stresses across the thickness of the shell. On the basis of shear deformation theory, Kabir and Chaudhuri[7] used a double Fourier series to obtain analytical solution of the free vibration of antisymmetrical angle-ply laminated shells. Soldatos[8] developed a refined shear deformable theory that accounts for parabolic variation of transverse shear strains and is capable of satisfying zero shear traction boundary conditions at the external shell or plate surface without making use of transverse shear correction factors. An approach based on Galerkin's method was used to solve the problem. Touratier[9] provided a generalized shear deformation theory for axisymmetrical multilayered shells. The shear forces were taken into account using "shear" functions introduced in the assumed kinematics. In the vibration and stability analyses of cross-ply laminated cylindrical shells, Nosier and Reddy[10] developed a new technique by generating Levy-type solutions and using an extension of Donnell's classical equations to first-order shear deformation theory.

In this Note, an improved general higher-order, thick-laminated-shell theory is established to analyze vibration of thick cylindrical shells. There are five unknowns in this theory, as in the first-order theory, but they have different physical meanings and include two additional rotations due to transverse shear forces. The theory is based on a summation of displacements of classic thin-shell theory and displacements due to transverse shear forces. The displacements due to transverse shear forces are in the form of cubic functions of the thickness coordinate that satisfy the parabolic distribution of the transverse shear stresses and zero transverse normal strain. The minimum total potential energy principle is used to obtain the frequencies of cylindrical shells. The effect of transverse shear force resultants on frequency characteristics has been studied by investigating the frequency variations with transverse shear correction factor K. Numerical results of the higher-order shear deformation theory and the first-order shear deformation theory are compared with existing results in the literature. The frequency characteristics for thick laminated composite cylindrical shells with different thickness-to-radius H/R and length-to-radius L/R ratios is presented

Received 26 April 1999; revision received 8 July 1999; accepted for publication 9 July 1999.

*Director and CEO, Institute of High Performance Computing, 89B Science Park Drive, 01-05/08, The Rutherford, Singapore Science Park 1.

†Principal Research Engineer, Institute of High Performance Computing, 89B Science Park Drive, 01-05/08, The Rutherford, Singapore Science Park 1.

‡Research Engineer, Institute of High Performance Computing, 89B Science Park Drive, 01-05/08, The Rutherford, Singapore Science Park 1.

for variations of circumferential wave number n and H/R and L/R ratios.

Theoretical Formulation

The geometry and coordinate system of the cylindrical shell under consideration is shown in Fig. 1. The cylindrical shell is of length L, thickness H, and radius R. Both of the ends of the shell are simply supported. The orthogonal curvilinear coordinate system (x, θ, z) is fixed at the middle surface of the cylindrical shell and x is the axial, θ is the circumferential, and z is the transverse coordinate.

In this Note, an improved higher-order theory is used to deal with the effect of shear forces on the frequencies of the cylinder. In higher-order shear deformation laminated theory, the Kirchhoff hypothesis is relaxed by removing the third part; i.e., the transverse normals do not remain perpendicular to the midsurface after deformation. The inextensibility of the transverse normals requires that w not be a function of the thickness coordinate z. The displacement field is assumed to be a combination of the displacements of classical thin-shell theory and the displacement caused by the transverse shear forces that satisfy zero transverse normal strains:

$$\begin{aligned} u(x, y, z) &= u_c(x, y, z) + u_s(x, y, z) \\ v(x, y, z) &= v_c(x, y, z) + v_s(x, y, z) \\ w(x, y, z) &= w_0(x, y, z) \end{aligned} \tag{1}$$

where

$$u_c = \left(1 + \frac{z}{R}\right)u_0 - z\frac{\partial w_0}{\partial x}, \qquad v_c = \left(1 + \frac{z}{R}\right)v_0 - z\frac{\partial w_0}{R\partial\theta}$$

$$u_s = \left(z^3 - \frac{zh^2}{4}\right)\varphi_x(x, y), \qquad v_s = \left(z^3 - \frac{zh^2}{4}\right)\varphi_\theta(x, y) \tag{2}$$

where u_c, v_c, and u_s, v_s are the displacements of classical thin-shell theory and displacements due to transverse shear forces, respectively; and φ_x and φ_θ are the rotations of transverse normal about the θ and x coordinates, respectively. In other words, these additional rotations are caused by the transverse shear forces.

The strains for a general shell are defined with respect to u, v, and w by

$$\begin{Bmatrix} \varepsilon_x \\ \varepsilon_\theta \\ \varepsilon_{\theta z} \\ \varepsilon_{xz} \\ \varepsilon_{x\theta} \end{Bmatrix} = \begin{Bmatrix} \dfrac{\partial u}{\partial x} + \dfrac{w}{R_1} \\ \dfrac{\partial v}{R_2\partial\theta} + \dfrac{w}{R_2} \\ \dfrac{\partial v}{\partial z} + \dfrac{\partial w}{R_2\partial\theta} - \dfrac{v_0}{R_2} \\ \dfrac{\partial u}{\partial z} + \dfrac{\partial w}{\partial x} - \dfrac{u_0}{R_1} \\ \dfrac{\partial v}{\partial x} + \dfrac{\partial u}{R_2\partial\theta} \end{Bmatrix} \tag{3}$$

where, for cylindrical shells, $R_1 = R$ and $R_2 = 0$.

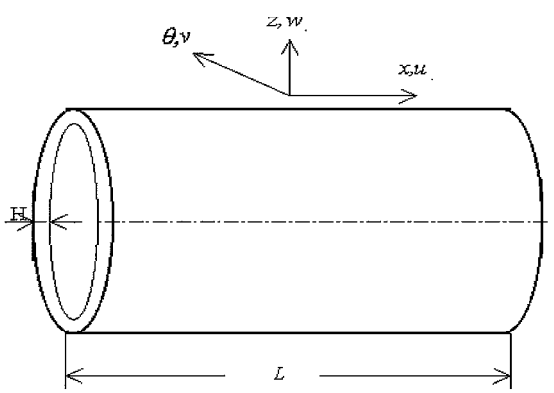

Fig. 1 Geometry and coordinate system of the cylindrical shell.

For cross-ply laminated shells, we obtain the transverse forces that are a parabolic distribution in the transverse direction while simultaneously satisfying the zero transverse strains on the top and bottom surfaces of the shell:

$$\begin{aligned} \sigma_{xz}(x, y, z) &= Q_{55}(z^2 - h^2/4)\varphi_\theta(x, y) \\ \sigma_{\theta z}(x, y, z) &= Q_{44}(z^2 - h^2/4)\varphi_x(x, y) \end{aligned} \tag{4}$$

For orthotropic layers the compliance matrix and stress-strain relation in the material coordinates are of the form

$$[S_{ij}] = \begin{bmatrix} 1/E_1 & -\nu_{21}/E_2 & 0 & 0 & 0 \\ -\nu_{12}/E_2 & 1/E_2 & 0 & 0 & 0 \\ 0 & 0 & 1/G_{23} & 0 & 0 \\ 0 & 0 & 0 & 1/G_{13} & 0 \\ 0 & 0 & 0 & 0 & 1/G_{12} \end{bmatrix}$$

$$\begin{bmatrix} \sigma_1 \\ \sigma_2 \\ \sigma_4 \\ \sigma_5 \\ \sigma_6 \end{bmatrix} = \begin{bmatrix} Q_{11} & Q_{12} & 0 & 0 & 0 \\ Q_{12} & Q_{22} & 0 & 0 & 0 \\ 0 & 0 & Q_{44} & 0 & 0 \\ 0 & 0 & 0 & Q_{55} & 0 \\ 0 & 0 & 0 & 0 & Q_{66} \end{bmatrix} \begin{bmatrix} \varepsilon_1 \\ \varepsilon_2 \\ \varepsilon_4 \\ \varepsilon_5 \\ \varepsilon_6 \end{bmatrix} \tag{5}$$

The coordinate system used in the solution of the problem does not coincide with the material coordinate system. Furthermore, these composite laminates have several layers, each with a different orientation of their material coordinates with respect to the laminate coordinates. Thus, we need to establish the transformation relations

$$[\bar{Q}] = [T][Q][T]^T \tag{6}$$

where $[T]$ is the standard transformation matrix.

Now we obtain the stress-strain relations in the problem coordinates:

$$\begin{Bmatrix} \sigma_x \\ \sigma_\theta \\ \sigma_{\theta z} \\ \sigma_{xz} \\ \sigma_{x\theta} \end{Bmatrix} = \begin{bmatrix} \bar{Q}_{11} & \bar{Q}_{12} & 0 & 0 & \bar{Q}_{16} \\ \bar{Q}_{12} & \bar{Q}_{22} & 0 & 0 & \bar{Q}_{26} \\ 0 & 0 & \bar{Q}_{44} & \bar{Q}_{45} & 0 \\ 0 & 0 & \bar{Q}_{45} & \bar{Q}_{55} & 0 \\ \bar{Q}_{16} & \bar{Q}_{26} & 0 & 0 & \bar{Q}_{66} \end{bmatrix} \begin{Bmatrix} \varepsilon_x \\ \varepsilon_\theta \\ \gamma_{\theta z} \\ \gamma_{xz} \\ \gamma_{x\theta} \end{Bmatrix} \tag{7}$$

The force and moment resultants for a thick shell are defined, respectively, by

$$\{N_x, N_\theta, N_{x\theta}\} = \sum_{k=1}^{N} \int_{z_{k+1}}^{z_k} \left\{\sigma_x\left(1 + \frac{z}{R}\right), \sigma_\theta, \sigma_{x\theta}\left(1 + \frac{z}{R}\right)\right\} \mathrm{d}z$$

$$\{M_x, M_\theta, M_{x\theta}\} = \sum_{k=1}^{N} \int_{z_{k+1}}^{z_k} \left\{\sigma_x\left(1 + \frac{z}{R}\right), \sigma_\theta, \sigma_{x\theta}\left(1 + \frac{z}{R}\right)\right\} z \, \mathrm{d}z$$

$$\{Q_x, Q_\theta\} = \sum_{k=1}^{N} \int_{z_{k+1}}^{z_k} \left\{\sigma_{xz}\left(1 + \frac{z}{R}\right), \sigma_{x\theta}\right\} z \, \mathrm{d}z \tag{8}$$

To avoid the complexity of the partial differential governing equations in terms of forces and moments, the frequencies of the shells are obtained by the minimum total potential energy principle. The strain energy U and the kinetic energy T for a thick cylindrical shell are defined as

$$U = \int_{-h/2}^{h/2} \int_0^L \int_0^{2\pi} (\sigma_x\varepsilon_x + \sigma_\theta\varepsilon_\theta + \sigma_{\theta z}\varepsilon_{\theta z} + \sigma_{xz}\varepsilon_{zx} + \sigma_{x\theta}\varepsilon_{x\theta}) R \, \mathrm{d}\theta \, \mathrm{d}x \, \mathrm{d}z$$

$$T = \frac{1}{2}\int_{-h/2}^{h/2} \int_0^L \int_0^{2\pi} \rho_t(\dot{u}^2 + \dot{v}^2 + \dot{w}^2) R \, \mathrm{d}\theta \, \mathrm{d}x \, \mathrm{d}z \tag{9}$$

$$\rho_t = \sum_{k=1}^{N} \int_{z_{k+1}}^{z_k} \rho^k z \, \mathrm{d}z \tag{10}$$

where ρ^k is the density per unit length of the kth laminate. The Lagrangian is

$$L = T_{\max} - U_{\max} \tag{11}$$

The displacement field is of the form

$$u_0 = A \cos px \cos n\theta e^{\omega t i}, \qquad v_0 = B \sin px \sin n\theta e^{\omega t i}$$

$$w_0 = C \cos px \sin n\theta e^{\omega t i}, \qquad \phi_x = D \cos px \cos n\theta e^{\omega t i}$$

$$\phi_\theta = E \sin px \sin n\theta e^{\omega t i} \tag{12}$$

where $p = m\pi/L$. The axial modal function has been chosen to be the simply supported characteristic beam modal function. For cross-ply laminated cylindrical shells, it can be seen from Eqs. (3), (8), and (12) that these assumed displacements satisfy simply supported boundary conditions, i.e., $w(0, L) = v(0, L) = N_x(0, L) = M_x(0, L) = \varphi_\theta(0, L) = 0$. Substituting Eqs. (3) and (12) into the Lagrangian of Eq. (11) and applying the minimum total potential energy principle, we obtain

$$\frac{\partial L}{\partial A} = \frac{\partial L}{\partial B} = \frac{\partial L}{\partial C} = \frac{\partial L}{\partial D} = \frac{\partial L}{\partial E} = 0 \tag{13}$$

Substituting the displacement field into Eq. (11) and applying Eq. (13) yields

$$\begin{bmatrix} C_{11} & C_{12} & C_{13} & C_{14} & C_{15} \\ C_{21} & C_{22} & C_{23} & C_{24} & C_{25} \\ C_{31} & C_{32} & C_{33} & C_{34} & C_{35} \\ C_{41} & C_{42} & C_{43} & C_{44} & C_{45} \\ C_{51} & C_{52} & C_{53} & C_{54} & C_{55} \end{bmatrix} \begin{Bmatrix} A \\ B \\ C \\ D \\ E \end{Bmatrix} = \begin{Bmatrix} 0 \\ 0 \\ 0 \\ 0 \\ 0 \end{Bmatrix} \tag{14}$$

Because the nontrivial solutions of a matrix equation are obtained only if the determinant of the matrix is zero, we obtain a fifth-order algebraic equation in ω^2, i.e., there are five pairs of distinct frequencies for every m-and-n combination. The roots of these equations are the natural frequencies, and the lowest of these five pairs of frequencies is associated with the mode where the transverse displacement component w_0 dominates.

Numerical Results and Discussion

To validate the present analysis, comparisons are made with existing results from the open literature. Present first-order and higher-order results for a long isotropic cylindrical thin shell are compared with results presented by Chen et al.[11] and Soedel[12] in Table 1. For a long thick cylindrical shell with simply supported boundary conditions, the corresponding comparisons are presented in Table 2. From the results presented in these two tables, it is observed that the present results agree well with those of Chen et al.[11] and Soedel.[12]

To prove the validity of this analysis for short shells ($L/R < 5$), comparisons are made with results presented by Timarci and Soldatos[13] for a short, thick, laminated cylindrical shells with simply supported boundary conditions. The results are presented in Table 3. The results of Timarci and Soldatos[13] are denoted by PAR (parabolic), HYP (hyperbolic), and UNI (uniform) and are the shear deformation shape functions used. PSDT is a parabolic shear deformable shell theory used by Timarci and Soldatos.[13] From the results in Table 3, we see that good agreement with other theories is attained for a very short, thick laminated cylindrical shell with simply supported boundary conditions.

This Note also compares at the frequency characteristic differences between thin and thick shells. Properties of the three-layered (0/90 deg/0) laminated composite cylindrical shell are $E_2 = 7.6 \times 10^9$ N/m^2, $E_1 = 2.5E_2$, $\rho = 1643$ kg/m^3, $\nu_{12} = 0.26$, $G_{12} = G_{13}, G_{23} = 0.2G_{12}$, and inner-, middle-, and outer-layer thickness $= h/3$. Figure 2 shows the variation of frequency parameter with n for the laminated composite cylindrical shell. The influences of the geometric properties h/R and L/R on the fundamental frequencies are presented in Figs. 3 and 4. From Fig. 2, it is observed that differences between the frequencies obtained by first-order and higher-order theories for a thick shell ($h/R = 0.2$) differ distinctly only when n becomes large. The corresponding numerical results are shown in Table 4. Table 5 shows corresponding results for a thin shell of $h/R = 0.002$, and here there is little difference between results from the two theories even at large n. From Fig. 3, which shows the variation of fundamental frequency parameter $(m, n) = (1, 1)$ for a thick shell with the h/R ratio for a laminated composite cylindrical shell, it is observed that the fundamental frequency parameters increase monotonically with the increase of the h/R ratio. This is unlike the case of a thin shell, where it is well known that the frequency parameters first decrease to a minimum before increasing monotonically. Because the circumferential wave number n considered in Fig. 3 is very small, the frequencies obtained by first-order

Table 1 Comparison of frequency parameter $\omega\sqrt{[\rho R^2(1-\nu_{12}^2)/E_2]}$ for a long cylindrical thin shell with simply supported boundary conditions ($m = 1$, $h/R = 0.002$, and $\nu = 0.3$)[a]

			Present	
n	Chen et al.[11b]	Soedel[12c]	First order	Higher order
2	0.00154919	0.00200014	0.00206636	0.00206636
3	0.00438178	0.00489912	0.00492965	0.00492965
4	0.00840168	0.00894441	0.00896183	0.00896183
5	0.0135873	0.0141423	0.0141533	0.0141533
6	0.0199323	0.020494	0.0205014	0.0205014
7	0.0274343	0.0280001	0.028005	0.028005
8	0.0360922	0.0366607	0.0366635	0.0366635

[a]First-order results obtained using shear correction factor of $\frac{5}{6}$.
[b]Equation of Chen et al.[11]:

$$\omega_{mn} = \sqrt{\frac{n^2(n^2-1)^2}{n^2+1} \frac{Eh^2}{\rho(1-\nu^2)12r^2}}$$

[c]Equation of Soedel[12]:

$$\omega_{mn} = \sqrt{\frac{E}{12\rho(1-\nu^2)} \frac{h^2}{r^2} \frac{1}{r^2} \left(\left(\frac{m\pi r}{L}\right)^2 + n^2\right)\left(\left(\frac{m\pi r}{L}\right)^2 + n^2 - 1\right)}$$

Table 2 Comparison of frequency parameter $\omega\sqrt{[\rho R^2(1-\nu^2)/E]}$ for a long cylindrical thick shell with simply supported boundary conditions ($m = 1$, $h/R = 0.2$, and $L/R = 200$)[a]

		Present	
n	Soedel[12]	First order	Higher order
1	0.000433617	0.0406152	0.0406152
2	0.200014	0.20207	0.202078
3	0.431542	0.469762	0.469858
4	0.793432	0.82573	0.826221
5	1.22304	1.25391	1.25551
6	1.70368	1.73985	1.74382
7	2.2221	2.27123	2.2794

[a]First-order results obtained using shear correction factor of $\frac{5}{6}$.

Table 3 Comparison of frequency parameter $\omega L^2\sqrt{(\rho E_2)/h}$ for a short laminated (0/90 deg/0) thick cylindrical shell with simply supported boundary conditions ($m = 1$, $h/R = 0.2$, $E_1/E_2 = 40$, $K = \frac{5}{6}$, $n = 2$, $G_{12} = 0.6E_2$, and $G_{23} = 0.5E_2$) against results of various theories used in Ref. 13[a]

Theory	$L/R = 1, n = 2$	$L/R = 2, n = 2$
Present	10.1438 (first) 10.0115 (higher)	18.8483 (first) 18.6943 (higher)
PAR	9.97	17.16
PSDT	10.07	17.77
HYP	9.99	17.16
UNI	9.99	17.16
CST	14.77	20.17

[a]First-order results obtained using shear correction factor of $\frac{5}{6}$.

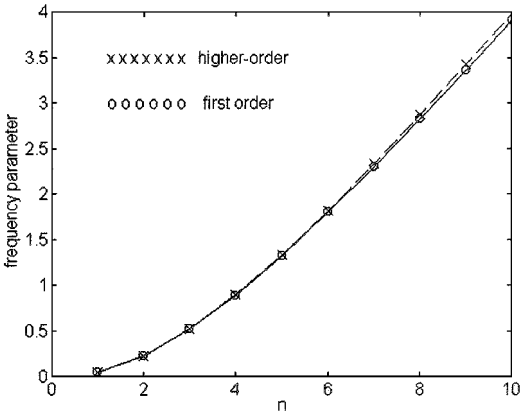

Fig. 2 Variation of frequency parameter $\omega\sqrt{[\rho R^2(1-\nu_{12}^2)/E_2]}$ with circumferential wave number n for a thick laminated composite cylindrical shell ($h/R = 0.2$, $L/R = 20$) for more $(m, n) = (1, 1)$. Shear correction factor of $\frac{5}{6}$ used for first-order results.

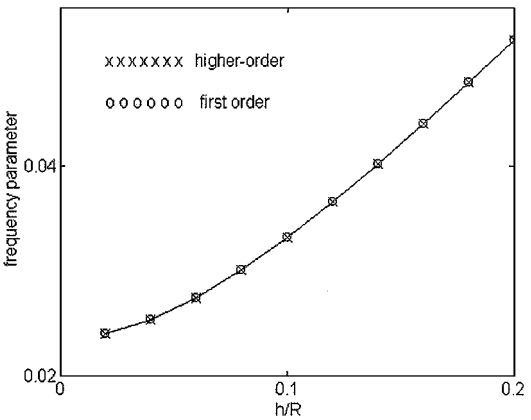

Fig. 3 Variation of frequency parameter $\omega\sqrt{[\rho R^2(1-\nu_{12}^2)/E_2]}$ with h/R ratio for a liminated composite cylindrical shell ($L/R = 20$). Shear correction factor of $\frac{5}{6}$ used for first-order results.

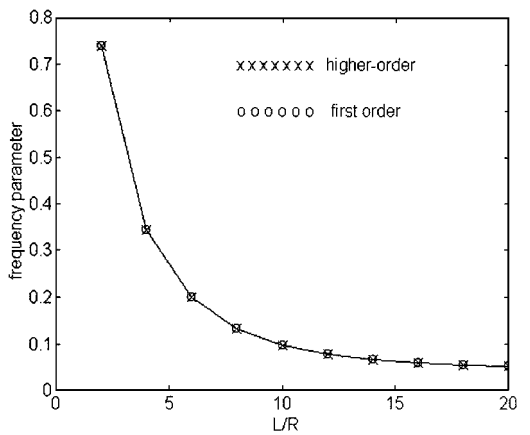

Fig. 4 Variation of frequency parameter $\omega\sqrt{[\rho R^2(1-\nu_{12}^2)/E_2]}$ with L/R ratio for a laminated composite cylindrical shell ($h/R = 0.2$) for mode $(m, n) = (1, 1)$. Shear correction factor of $\frac{5}{6}$ used for first-order results.

and higher-order theories have minimal differences even though we are considering the case of a thick shell. This is in line with the conclusions of Fig. 2. Table 6 presents the corresponding numerical results of Fig. 3. Figure 4 shows that, for mode $(m, n) = (1, 1)$, as the L/R ratio increases, the frequencies decrease. This is intuitively correct because the stiffness decreases with the increase in length. Also, the L/R ratio is not a contributing factor to differences in the frequency parameters arising from results between first-order theory and higher-order theories. In corresponding results presented in Table 7, the minimal differences can be clearly seen.

Table 4 Variation of frequency parameter $\omega\sqrt{[\rho R^2(1-\nu_{12}^2)/E_2]}$ with circumferential wave number n for a thick laminated composite cylindrical shell ($h/R = 0.2$ and $L/R = 20$) and axial mode $m = 1$

n	Higher order	First order
1	0.0519432	0.0519305
2	0.226436	0.22613
3	0.515465	0.517007
4	0.887824	0.892341
5	1.32054	1.33044
6	1.79558	1.81368
7	2.29945	2.32873
8	2.82243	2.86585
9	3.35773	3.41804
10	3.90064	3.98034

Table 5 Variation of frequency parameter $\omega\sqrt{[\rho R^2(1-\nu_{12}^2)/E_2]}$ with circumferential wave number n for a thin laminated composite cylindrical shell ($h/R = 0.002$ and $L/R = 20$) and axial mode $m = 1$

n	Higher order	First order
1	0.0235941	0.0235941
2	0.0080821	0.0080821
3	0.0066802	0.0066802
4	0.0103551	0.0103551
5	0.0160583	0.0160583
6	0.0231884	0.0231883
7	0.0316499	0.0316499
8	0.0414232	0.0414231
9	0.0525028	0.0525027
10	0.064887	0.0648867

Table 6 Variation of frequency parameter $\omega\sqrt{[\rho R^2(1-\nu_{12}^2)/E_2]}$ with h/R ratio for a laminated composite cylindrical shell ($L/R = 20$) and mode $(m, n) = (1, 1)$

h/R	Higher order	First order
0.02	0.0240473	0.0240473
0.04	0.0253702	0.0253702
0.06	0.0274308	0.0274306
0.08	0.0300737	0.0300731
0.10	0.033155	0.0331538
0.12	0.0365583	0.0365559
0.14	0.0401953	0.0401913
0.16	0.0440013	0.0439951
0.18	0.0479289	0.0479198
0.20	0.0519432	0.0519305

Table 7 Variation of frequency parameter $\omega\sqrt{[\rho R^2(1-\nu_{12}^2)/E_2]}$ with L/R ratio for a laminated composite cylindrical shell ($h/R = 0.2$) and mode $(m, n) = (1, 1)$

L/R	Higher order	First order
2	0.738969	0.739281
4	0.343537	0.343607
6	0.199428	0.199481
8	0.132266	0.132312
10	0.0970384	0.097081
12	0.0773196	0.0773594
14	0.0658263	0.0658638
16	0.0589203	0.0589559
18	0.0546536	0.0546878
20	0.0519432	0.0519765

Table 8 Variation of frequency parameter $\omega\sqrt{[\rho R^2(1-\nu_{12}^2)/E^2]}$ with K for thin ($h/R = 0.002$) and thick ($h/R = 0.2$) laminated composite shells

	$h/R = 0.002$			$h/R = 0.2$		
K	$n = 1$	$n = 3$	$n = 5$	$n = 1$	$n = 3$	$n = 5$
0	0.0235895	0.00366906	0.00136952	0.0236306	0.00367662	0.00137238
0.1	0.0235941	0.00667993	0.0160559	0.0496758	0.373063	0.761253
0.2	0.0235941	0.00668007	0.0160573	0.0509063	0.437051	0.968167
0.3	0.0235941	0.00668012	0.0160577	0.0513454	0.466859	1.08537
0.4	0.0235941	0.00668014	0.0160579	0.0515708	0.484197	1.16201
0.5	0.0235941	0.00668015	0.0160581	0.0517079	0.495553	1.21627
0.6	0.0235941	0.00668016	0.0160582	0.0518002	0.503573	1.25677
0.7	0.0235941	0.00668017	0.0160582	0.0518665	0.509539	1.28818
0.8	0.0235941	0.00668018	0.0160583	0.0519165	0.514151	1.31327
0.9	0.0235941	0.00668018	0.0160583	0.0519555	0.517824	1.33376
1	0.0235941	0.00668018	0.0160583	0.0519868	0.520818	1.35082
HSDT[a]	0.0235941	0.00668018	0.0160583	0.0519432	0.515465	1.32054

[a]HSDT, Higher-order shear deformation theory.

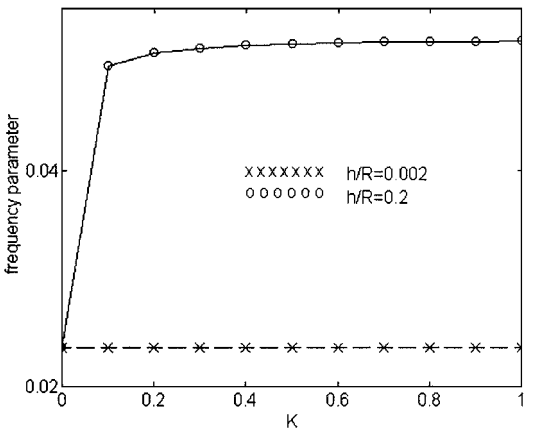

Fig. 5 Variation of frequency parameter $\omega\sqrt{[\rho R^2(1-\nu_{12}^2)/E_2]}$ with transverse shear correction factor K for a thin ($h/R = 0.002$) and a thick ($h/R = 0.2$) laminated composite shell for mode $(m, n) = (1, 1)$.

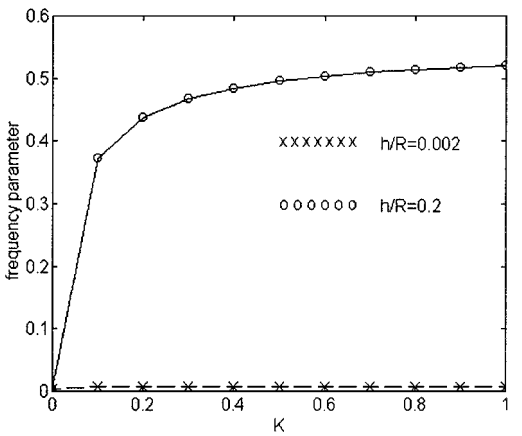

Fig. 6 Variation of frequency parameter $\omega\sqrt{[\rho R^2(1-\nu_{12}^2)/E_2]}$ with transverse shear correction factor K for a thin ($h/R = 0.002$) and a thick ($h/R = 0.2$) laminated composite shell for mode $(m, n) = (1, 3)$.

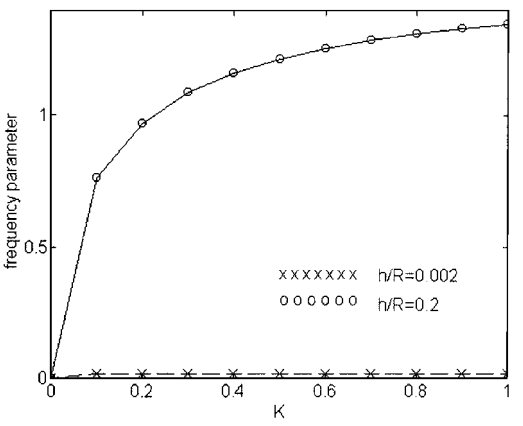

Fig. 7 Variation of frequency parameter $\omega\sqrt{[\rho R^2(1-\nu_{12}^2)/E_2]}$ with transverse shear correction factor K for a thin ($h/R = 0.002$) and a thick ($h/R = 0.2$) laminated composite shell for mode $(m, n) = (1, 5)$.

The frequencies of short, thick shells obtained from many shell theories diverge when the circumferential wave number n decreases from a large value to 1. Because first-order theory provides simpler ways to solve this kind of problem, the accuracy and selection of the transverse shear correction factor K becomes an important issue. Basically, the sensitivity of frequencies to the transverse shear correction factor K is of interest here, and the present study identifies situations where one should be more careful in selecting a K value. The shear correction factor is introduced to resolve the discrepancy between the actual stress state and the constant-stress state predicted by the first-order theory, where it is used to compute the transverse shear force resultants by multiplying the relevant integrals with K. Figures 5, 6, and 7 show the variation of fundamental frequency parameter with transverse shear correction factor K for thin ($H/R = 0.002$) and thick ($H/R = 0.2$) laminated composite shells with circumferential wave number $n = 1$, 3, and 5, respectively, and the corresponding numerical results are presented in Table 8. It can be seen that, when K is zero, the frequency parameters of the thick shell and the thin shell cannot be distinguished. In other words, if the influence of the transverse shear force resultants is neglected, the frequencies of a thick shell and a corresponding thin shell are almost similar. Figures 5–7 also show that the larger the circumferential wave number n is, the more difficult it is for the frequency parameters to converge with respect to K, i.e., the more important is the selection of the K value. From Table 8, which presents results for a thick shell, the results obtained by the higher-order theory are generally between the results obtained by first-order theory using values of $K = 0$ and 1. On further inspection, for $n = 1$, the results obtained by the higher-order theory are equivalent to the results of the first-order theory using K between 0.8 and 0.9. For $n = 3$ and 5, the higher-order-theory results are equivalent to results of first-order theory using K between 0.8 and 0.9. Thus, on the basis of higher-order theory, the transverse shear correction factor K may not be a constant, at least with respect to the circumferential wave number n.

Conclusions

A higher-order shear deformation theory of laminated shell is presented. The displacement is based on the summation of the displacements of classic thin shell theory and those due to transverse shear forces. The five independent unknowns are the same in number as with the first-order theory, but they have different physical meanings. The displacements due to transverse shear forces are assumed to be in the form of cubic functions so that they satisfy

the parabolic distribution of the transverse shear stresses and zero transverse normal strain on the top and bottom surfaces of the shells. Exact solutions for thick cross-ply laminated cylindrical shells are presented by applying the minimum total potential energy principle. A study on how transverse shear force resultants affect the frequency characteristic by investigating the frequency variations with transverse shear correction factor K is also presented. On the basis of higher-order theory, the transverse shear correction factor K was found to be nonconstant as the circumferential wave number n was varied.

References

[1]Donnell, L. H., "Stability of Thin Walled Tubes Under Torsion," NACA Rept. 479, 1933.

[2]Love, A. E. H., *Treatise on the Mathematical Theory of Elasticity*, Dover, New York, 1944, Chap. 24.

[3]Flugge, W., *Stresses in Shells*, Springer-Verlag, Berlin, 1962.

[4]Reddy, J. N., "A Simple Higher-Order Theory for Laminated Composite Plates," *Journal of Applied Mechanics*, Vol. 51, Dec. 1984, pp. 745–752.

[5]Soldatos, K. P., and Hadjigeorgiou, V. P., "Three-Dimensional Solution of the Free Vibration Problem of Homogeneous Isotropic Cylindrical Shells and Panels," *Journal of Sound and Vibration*, Vol. 137, No. 3, 1990, pp. 369–384.

[6]Voyiadjis, G. Z., and Shi, G. Y., "A Refined Two-Dimensional Theory for Thick Cylindrical Shells," *International Journal of Solids and Structures*, Vol. 27, No. 3, 1989, pp. 261–282.

[7]Kabir, H. R. H., and Chaudhuri, R. A., "Free Vibration of Shear-Flexible Anti-Symmetric Angle-Ply Doubly Curved Panels," *International Journal of Solids and Structures*, Vol. 28, No. 1, 1991, pp. 17–32.

[8]Soldatos, K. P., "A Refined Laminated Plate and Shell Theory with Applications," *Journal of Sound and Vibration*, Vol. 144, No. 1, 1991, pp. 109–129.

[9]Touratier, M., "A Generalization of Shear Deformation Theories for Axisymmetric Multilayered Shells," *International Journal of Solids and Structures*, Vol. 29, No. 11, 1992, pp. 1379–1399.

[10]Nosier, A., and Reddy, J. N., "Vibration and Stability Analyses of Cross-Ply Laminated Circular Cylindrical Shells," *Journal of Sound and Vibration*, Vol. 157, No. 1, 1992, pp. 139–159.

[11]Chen, Y., Zhao, H. B., and Shen, Z. P., "Vibrations of High Speed Rotating Shells with Calculations for Cylindrical Shells," *Journal of Sound and Vibration*, Vol. 160, No. 1, 1993, pp. 137–160.

[12]Soedel, W., *Vibrations of Shells and Plates*, Marcel Dekker, New York, 1993, Chap. 12.

[13]Timarci, T., and Soldatos, K. P., "Comparative Dynamic Studies for Symmetric Cross-Ply Circular Cylindrical Shells on the Basis of a Unified Shear Deformable Shell Theory," *Journal of Sound and Vibration*, Vol. 187, No. 4, 1995, pp. 609–624.

A. N. Palazotto
Associate Editor